ARTICLE

Power Balance Control Strategy of Cascaded H-Bridge Multilevel Inverter Based on Improved Harmonic Injection

Feng Zhao, Haonan Xu*, Xiaoqiang Chen and Ying Wang

School of Automation and Electrical Engineering, Lanzhou Jiaotong University, Lanzhou, 730070, China

*Corresponding Author: Haonan Xu. Email: xhnlajt2025@163.com

ABSTRACT: The cascaded H-bridge (CHB) multilevel inverter has become one of the most widely used PV inverter topologies due to its high voltage processing capability and high quality output power. Grid-connected PV system due to external conditions such as PV panel shading, PV component damage, can lead to PV output power imbalance, triggering the system over-modulation phenomenon, which in turn leads to grid-connected current waveform distortion. To this end, an improved power balance control strategy is proposed in this paper. Firstly, according to the different modulation ratios of each H-bridge module, a suitable harmonic injection method is used to keep the peak value of the modulating waveform always at 1; then an inverse triangular trapezoidal waveform is injected to optimize the modulating waveform, which further improves the output voltage waveform, reduces the THD value of the grid-connected currents, and maintains the stability of power inside the CHB system. Purpose. Simulation verifies the effectiveness and feasibility of this power balance control strategy.

KEYWORDS: Cascaded H-bridge inverter; harmonic injection; inverse triangular trapezoidal waveform; power balance control

1 Introduction

In order to alleviate the pressure of growing energy demand without damaging the environment, in recent years, the share of renewable energy sources (e.g., solar, ocean, and wind) in the power system has been increasing annually, and has gradually become an important direction to promote the transformation of the energy structure. Among them, solar power is regarded as one of the fastest-growing and most promising green energy sources due to its low carbon emissions and non-pollution advantages.

With the rapid construction of small, medium and large-scale photovoltaic (PV) power plants, PV systems are facing many challenges, including how to improve PV utilisation, optimise the stability of grid-connected currents to meet the demands of user loads, and prolonging the service life of the equipment. Therefore, it is of great significance to study and propose effective strategies to solve these problems in order to realise the wide application of PV power generation [1].

The cascaded H-bridge multilevel inverter (CHB) is widely used as the preferred topology in modern grid-connected PV systems due to its modularity, high reliability, high efficiency and good power quality. Compared with the traditional two-level inverter, the cascaded H-bridge multilevel inverter can output multilevel through step-wave modulation, which significantly reduces the harmonic content in the output current.

The filter design adopts a single inductor output structure, which can effectively avoid the resonance risk of LCL filter. Using low-voltage and high-efficiency modular technology, this topology significantly improves the reliability of the system and makes it easy to achieve large-scale production. The design feature of no frequency transformer enables the output current to be directly connected to the medium voltage grid, simplifying the system structure and reducing the nighttime power consumption of the PV inverter to a certain extent [2,3].

External environmental factors (e.g., cloud cover, dust or leaves on the surface of the PV panel) can lead to uneven light intensity received by the PV module, triggering a power imbalance. At the same time, module failure can also cause the switch between it and the H-bridge to be disconnected, resulting in an imbalance in the power generated by the cascaded H-bridge. Both of these situations trigger the phase-to-phase power imbalance problem in the three-phase CHB PV grid-connected inverter. The H-bridge unit corresponding to the PV module with higher output power may be at risk of over-modulation, which increases the harmonic components of the grid current, affects the quality of the grid-connected current, and, in severe cases, causes system instability.

In order to solve the power imbalance phenomenon caused by external environmental problems, in-depth research has been carried out at home and abroad for this problem. Literature [4] proposed a new concept of identical modular magnetic chain using third harmonic injection 60-degree bus-clamped pulse width modulation (PWM) technique, which has better spectral characteristics can improve the quality of grid-connected current and reduce switching losses, but there are still more high harmonics. Literature [5] proposed a third harmonic injection equal load 90 degree clamped PWM (THELNDCPWM) technique which can reduce the total harmonic distortion (THD) and power loss during SMES discharge. Literature [6–8] achieved mutual cancellation of harmonic components in the total output voltage by introducing multiple harmonic components in the overmodulation module and injecting reverse harmonics in the non-overmodulation module, which extends the linear modulation range of the system from 1.155 to 1.270, but the active power of the high power H-bridge fails to fully utilise its maximum output potential. Literature [9,10] proposed a novel harmonic compensation control method by injecting an appropriate amount of fundamental waveform components into the modulating waveforms of the overmodulated units and injecting the 3rd and 5th harmonics to ensure that the peak value of the modulating waveforms is always maintained at 1. At the same time, in order to avoid the un-overmodulated units to trigger the reverse overmodulation due to the initial harmonic injections, the reverse harmonic components are introduced to these units, which avoids the instability of the system. Literature [11] proposed an advanced PWM technique to improve the linear modulation range by injecting square waves to achieve the minimum compensation to reduce the power loss and voltage THD. Literature [12] proposed a hybrid photovoltaic-storage power routing based on the cascaded H-bridge (CHB) structure, which is efficiently achieved by configuring a small number of storage modules in a three-phase CHB PV inverter and utilising the synergistic PV and storage control strategy to maintain the internal power balance of the CHB system. Literature [13] proposes a power balance control strategy with a dual min-max zero-sequence injection method, clarifies the generation mechanism of the power imbalance problem based on the voltage-current vector diagram of the inverter, and analyses and compares the composition of different zero-sequence injection methods and their implementation methods. Literature [14] proposes an Modified Modulation Waveform Injection Strategy (MMWIS), in which the fine-tuning quantity in the traditional modulated waveform injection strategy is improved by taking a part of the difference between the square waveform with amplitude ±1 and in phase with the current and the modulated waveform as the fine-tuning quantity, so as to extend the maximum modulation ratio of the high-power module to $\pi/4$, and make its output active power reach the maximum value of the output it is able to produce. Literature [15] proposes a trapezoidal wave compensation control method. When the system operates beyond the linear modulation region of trapezoidal wave compensation, the power adaptive

control strategy is used to dynamically adjust the output power of the front-stage microsource, thus effectively preventing the occurrence of over-modulation phenomenon.

Existing studies have proposed a variety of power balance control strategies for power imbalance conditions, and although the grid-connected current distortion is effectively suppressed, the total harmonic distortion (THD) of the system grid-connected current is still significantly higher than that of the power balance state under non-ideal operating conditions. Therefore, it is still necessary to further improve the grid-connected power quality by optimising the modulating waveform.

In this paper, an improved power balance control strategy is proposed, which adopts different harmonic compensation strategies according to the difference of modulation ratios of each H-bridge module, and at the same time injects the inverse triangular trapezoidal waveform into the modulating waveform to change the amplitude distribution of the waveform, so that the modulating waveform shape is more uniform, and achieves the purpose of reducing the THD value of the grid-connected current and the loss of the system. A three-phase seven-level solar photovoltaic grid-connected system is designed based on cascaded H-bridge topology and the proposed power balance control strategy is analysed in terms of total harmonic distortion (THD) of the grid-connected current.

2 Improved Power Balance Control Strategy and Mathematical Model Analysis

2.1 Analysis of Single-Phase Cascaded H-Bridge Mathematical Model

Fig. 1 shows the CHB PV grid-connected inverter topology with A-phase as an example, each H-bridge module Comprises four switching tubes ($S_{x1} - S_{x4}$), and the AC side is connected to the grid via the filter inductor. $V_{\mathrm{PV}x}$ and $I_{\mathrm{PV}x}$ are the output voltage and output current of the PV module on the DC side of the xth module, respectively; C_x is the filter capacitor, I_{Cx} is the current of the corresponding filter capacitor; $I_{\mathrm{H}x}$ and $U_{\mathrm{dc}x}$ are the DC side current and voltage of each H-bridge unit; $U_{\mathrm{H}x}$ is the AC output voltage of each H-bridge unit; U_g and I_g are the grid voltage and grid current, respectively; L_{S} is the filter inductor, and U_L is the corresponding filter inductor voltage.
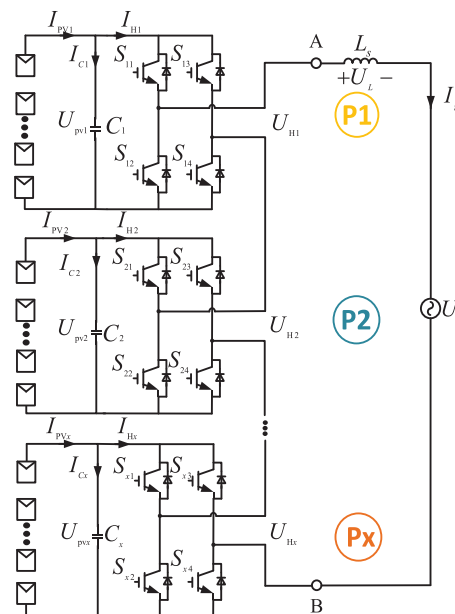

Figure 1: Topology of A-phase CHB photovoltaic grid-connected inverter

The outputs of the cascaded H-bridge are connected in series, and due to shading of the PV panels or damage to the PV modules, the output power of the PV modules belonging to the cascaded H-bridge decreases, leading to a reduction in the total output power P_T. The grid voltage V_g of the system remains constant, which causes a drop in the grid current I_g of the cascaded H-bridge inverter, this consequently triggers a failure in maximum power point tracking (MPPT).

Under this condition, for the H-bridge module with changing output power, Voltage compensation is required for the H-bridge module with varying output power. However, overcompensation would increase the modulating waveform amplitude, resulting in system overmodulation, and the system will be overmodulated.

The modulating wave A for the number M_x-th H-bridge unit during the stable operation of the inverter can be defined as:

$$M_x = U_{Hx}/U_{dcx} \tag{1}$$

According to Kirchhoff's law, the mathematical model of the AC side can be expressed as follows, ignoring line resistance and switching losses:

$$L_s dI_g/dt = U_{AB} - U_g \tag{2}$$

$$U_{AB} = U_{H1} + U_{H2} + \cdots + U_{Hx} \tag{3}$$

Combining Eqs. (1)–(3) gives:

$$L_s \frac{dI_g}{dt} = \sum_{x=1}^{n} m_x U_{dcx} - U_g \tag{4}$$

Eq. (4) can be rewritten by means of vector analysis as:

$$j\omega L_s \boldsymbol{I}_g = \sum_{x=1}^{n} \boldsymbol{M}_x U_{dcx} - \boldsymbol{U}_g \tag{5}$$

where $\boldsymbol{U}_g$, $\boldsymbol{I}_g$, $\boldsymbol{M}_x$ are the phase forms of U_g, I_g, m_x, respectively, and ω is the angular frequency.

As depicted in the vector diagram of Fig. 2, when the inverter operates at unit power factor, the voltage component U_L of the filter inductor L_s is much smaller than the grid voltage U_g, and therefore the modulation phase angle δ is close to 0, which can be approximated as $\cos\delta \approx 1$. This reduces the transmission of reactive power, reduces the line losses, and improves the system efficiency.
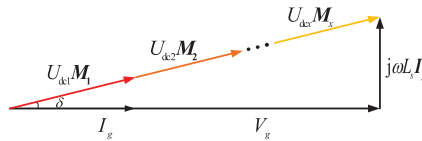

Figure 2: Phasor diagram of CHB operating at unity power factor

2.2 Stability Domain Range Analysis

During unit power factor operation, the peak value of the modulating wave for each unit is less than 1. At this time, the amplitude of the modulating wave is $M_x \leq \sqrt{2}/2$, which is the basic requirement to ensure the stable operation of the CHB grid-connected inverter.

The active power injected into the grid by the x-th H-bridge unit is expressed as:

$$P_{\mathrm{H}x} = U_{\mathrm{H}x}I_g = |U_{\mathrm{dc}x}M_x||I_g|\cos\delta \approx U_{\mathrm{dc}x}|M_x||I_g| \tag{6}$$

where $U_{\mathrm{H}x}$ is the AC-side output voltage of the x-th H-bridge module, I_g is the grid-connected current, M_x is the modulating wave amplitude of the x-th H-bridge unit, and $U_{\mathrm{dc}x}$ is the DC-side input voltage of the x-th H-bridge module.

Define the active power on the DC side of the x-th H-bridge to be expressed as:

$$P_x = U_{\mathrm{dc}x}I_{\mathrm{PV}x} \tag{7}$$

where $I_{\mathrm{PV}x}$ is the x-th PV panel output current. Based on the equality of the transmitted power on the AC side and the DC side, and based on $M_x \leq \sqrt{2}/2$ the condition to avoid the occurrence of over-modulation can be obtained:

$$U_{\mathrm{dc}x}I_{\mathrm{PV}x} = U_{\mathrm{dc}x}M_xI_g \tag{8}$$

That is, the RMS value of the grid current is not less than the times of the output current of each PV module, i.e., $I_g \geq \sqrt{2}I_{\mathrm{PV}x}$, This inequality constitutes a necessary condition for grid stability. Satisfying this relationship, the peak value of the modulating wave of the system will be limited to within 1, when the system works in the linear modulation region.

2.3 Improved Power Balance Control Strategy

It has been investigated to extend the effective linear modulation range of the inverter to 1.270 by means of harmonic compensation control strategy. The power balance control strategy proposed in this paper achieves the optimisation of the modulation waveform by dynamically adjusting the modulation ratio of each H-bridge unit.

As shown in Table 1, according to the size of the modulation ratio, the system operating region is divided into four stages, and different harmonic compensation methods are used in each stage.

Table 1: Modulation wave operation modes under different operating conditions

Modulation range	Working method
0–1.000	Proper functioning
1.000–1.115	Third harmonic compensation
1.115–1.207	Fifth harmonic compensation
1.207–1.270	Fundamental compensation (physics)

Combined with the inverse triangular trapezoidal waveform injection method in the power balance state proposed in the literature 18, this study extends it to the power imbalance state, and achieves synergistic control of harmonic compensation and waveform optimisation by adjusting the phase and amplitude of the injected waveform, which further reduces the THD value of the grid-connected current. Good results are also demonstrated through simulation.

Fig. 3 shows a schematic diagram of the 3rd harmonic compensation, where a synthetic modulating waveform m_1 is generated by injecting the 3rd harmonic $m_{\mathrm{T}1}$ into the initial modulating waveform m_{a1} when

the modulation ratio is 1.115. This strategy achieves an output capability with an equivalent modulation ratio of 1.115 while ensuring that the peak value of the modulating waveform does not exceed 1.
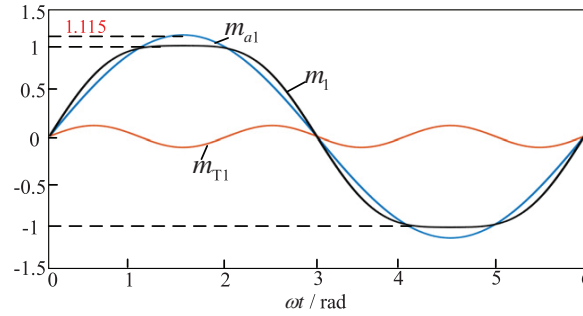

Figure 3: Schematic diagram of third harmonic injection

The synthesised modulated wave m_1 can be expressed as:

$$m_1 = M_x sin\,(\omega t + \delta) + k_x\,\,sin\,(3\omega t + 3\delta) \tag{9}$$

Fig. 4 shows the schematic after injecting the 3rd and 5th harmonics into the modulating wave of the overmodulation unit, at which point the system reaches a linear modulation range of 1.270.
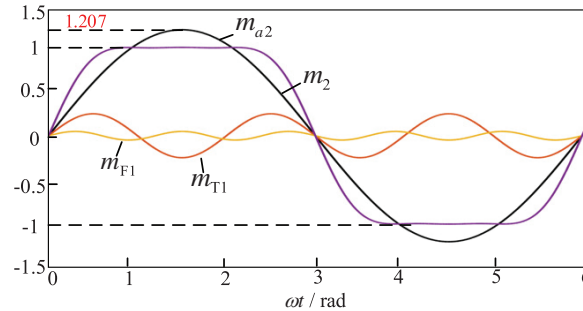

Figure 4: Schematic diagram of third and fifth harmonic injection

In Fig. 4, m_2 is the modulated waveform before compensation, and m_{T1} and m_{F1} are the compensated 3rd and 5th harmonics. It can be seen that the synthesised m_2 reaches a peak value of 1.207 for m_{a2} while ensuring that the peak value is not greater than one.

The modulated wave m_{a2} of the xth cell obtained after compensation can be expressed as:

$$m_{a2} = M_x sin\,(\omega t + \delta) + k_x\,\,sin\,(3\omega t + 3\delta) + l_x\,\,sin\,(5\omega t + 5\delta) \tag{10}$$

Fig. 5 shows the fundamental compensation method, by introducing an appropriate amount of inverted fundamental wave into the overmodulation unit, this mode is used for modulation ratios in the range of 1.207–1.270.

In the figure, m_3 is the total modulated waveform before compensation and m_{p1} is the compensated fundamental frequency modulated waveform. Then the modulating wave m_{a3} in the x-th cell can be expressed as:

$$m_{a3} = M_x\,\,sin\,(\omega t + \delta) + k_x\,\,sin\,(\omega t + \delta) \tag{11}$$
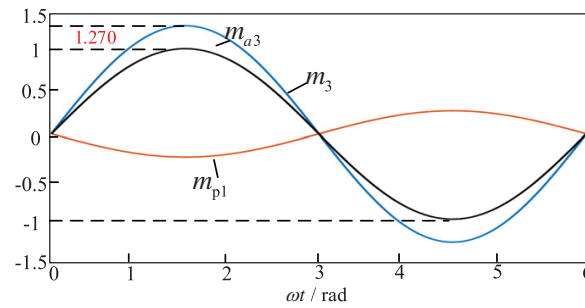
Figure 5: Schematic diagram of fundamental wave injection

The methods of harmonic compensation under different modulation regimes are given in Figs. 3–5. Different light intensity causes different modulation ratios for different H-bridge modules, so different harmonic compensation control strategies are used for different H-bridge modules in case of system power imbalance.

For the non-over-modulated units need to compensate for an equal amount of inverse harmonics, and the compensation of inverse harmonics raises the peak value of the modulating waveform to 1 to further improve the quality of the output current waveform.

On the basis of the harmonic compensation control strategy mentioned above, the triangle wave saturation common mode control strategy proposed in reference [16] is integrated. As shown in Fig. 6, the CHB injects multiple harmonics and then injects an inverse triangular-trapezoidal waveform to improve the linearity and harmonic characteristics of the output voltage by optimising the shape of the modulating waveform, increase the effective output voltage by changing the peak position of the modulating waveform, reduce the amplitude of the low-frequency harmonics, and concentrate the high-frequency harmonics in a higher frequency band, eliminating the influence of the high-frequency subharmonics, which is easy to be suppressed by a filter.
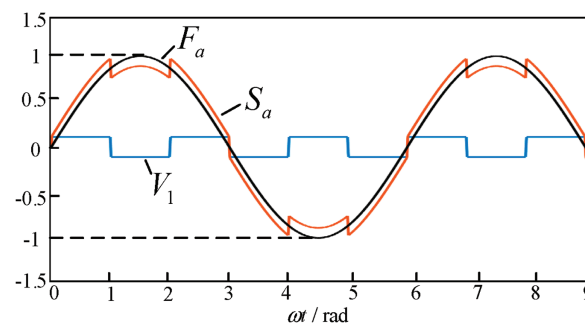

Figure 6: The triangular-trapezoidal wave injection strategy

The specific implementation method is as follows, the modulating waveform is sinusoidal modulating signal F_a:

$$F_a = A \sin(\omega t) \tag{12}$$

where A is the modulating wave amplitude, according to the amplitude phase of the modulating wave to generate an inverse triangular wave, by limiting the amplitude to within ±0.11C to obtain an inverse triangular trapezoidal wave V_2.

$$V_1 = 2\pi C * \sin^{-1}\left\{\sin\left(3\omega t\right)\right\} \tag{13}$$

$$V_1 = V_2$$

$$\begin{aligned}
&= 0.11C \left(\text{if } V_1 > 0.11C\right)\\
&= -0.11C \left(\text{if } V_1 < -0.11C\right)
\end{aligned} \tag{14}$$

where $C = 0.77A$, from which the modulated signal S_a can be obtained after injecting the inverse triangular trapezoidal waveform:

$$S_a = F_a + V_2 \tag{15}$$

3 System Control Block Diagram Analysis

3.1 Voltage-Current Double Closed-Loop Overall Control Strategy

The overall control structure of the three-phase CHB seven-level PV grid-connected inverter is shown in Fig. 7, including three parts: the MPPT control, the voltage-current dual-loop control and the improved power balance control. Among them, the independent MPPT control algorithm adopts the conductance increment method, which is simple to implement and can effectively reduce the power fluctuations near the maximum power point, showing good control performance.
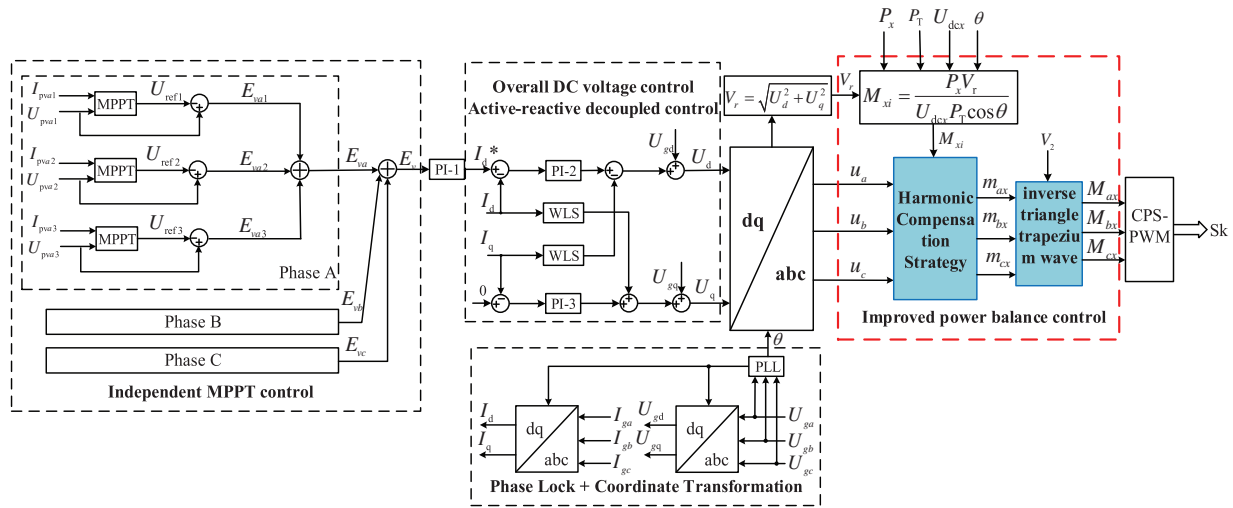

Figure 7: System control block diagram

The voltage outer loop adopts the overall DC-side voltage error control, the DC-side voltage control through the independent decoupling of active and reactive currents of the inverter, the control purpose is to make U_{pv} track the MPP at any time. The sum of the DC-side voltage error E_v adopts the PI control in order to keep the overall dc-side voltage stable outputs to get the d-axis current reference value I_d*. When the inverter operates stably at unit power factor, its reactive power is 0, so the grid-connected current reactive reference value is equal to 0. I_d and I_q are the active and reactive feedback quantities of the current in the dq coordinate system. The reference values I_d* and I_q*, and the feedback quantities I_d and I_q are regulated by the PI of the inner loop to produce the active and reactive control quantities V_d and V_q.

3.2 Calculation of Modulated Waves

Equations in display format should be separated from the surrounding text, aligned to the left of the column, with the equation label aligned to the right margin. Equations must be editable and numbered consecutively in Arabic numerals within parentheses, where applicable. See Eq. (1) for an example:

The inner loop outputs the co-modulation ratio M_{xi} and the co-modulation signal angle θ, respectively:

$$M_{xi} = \frac{P_x V_r}{u_{dcx} P_T \cos \theta} \tag{16}$$

$$\theta = \arctan \frac{V_d}{V_q} \tag{17}$$

where V_r can be expressed as:

$$V_r = \sqrt{U_d^2 + U_q^2} \tag{18}$$

The modulated waveform m_{a2} consists of two components, the initial fundamental frequency modulated waveform and the compensating harmonics, i.e.,

$$m_{a2} = f_x + T_x \tag{19}$$
$$f_x = M_{xi} \sin(\omega_0 t + \theta) \tag{20}$$

where m_{a2} is the H-bridge modulating signal after the third and fifth harmonics are injected, refer to Eq. (10). Where T_x is the compensated 3rd and 5th harmonics and f_x is the fundamental signal. Finally, the final modulating waveform M_{ax} is obtained by injecting the inverse triangular trapezoidal waveform V_2 with reference to Eqs. (13) and (14), and the expression is:

$$M_{ax} = m_{a2} + V_2 \tag{21}$$

4 Simulation and Result Analysis

The Institute of Electrical and Electronics Engineers (IEEE) has issued a standard that recommends that the total harmonic distortion (THD) of the grid-connected current should not exceed 5% for low-voltage equipment connected to the public power grid.

In order to verify the feasibility and effectiveness of the power balance control strategy of the three-phase cascaded H-bridge PV grid-connected inverter proposed in this paper, a Simulink simulation model of a seven-level PV grid-connected system with a cascade of three H-bridge units is constructed with the specific parameters of the circuits as shown in Table 2 and the parameters of the PV modules as shown in Table 3.

Table 2: Simulation parameter settings

Parametric	Numerical value
Number of cascade units n	3
Switching frequency f_c/kHz	1
Grid voltage U_s/V	220
Filter Inductors L_s/mh	2
DC side shunt capacitor C_x/mF	4

Table 3: PV module parameter settings

Parametric	Numerical value
Maximum output power P_{xmax}/W	6300
Open circuit voltage U_{oc}/V	216
Maximum power point voltage U_{mpp}/V	205
Maximum power point current I_{mpp}/A	30.7
Short-circuit current I_{sc}/A	35

Simulation Verification

In the simulation setup, the PV panel temperature and solar radiation intensity of the three units are the same at the initial moment, and the solar radiation intensity is set to 1000 W/m² to ensure that the input power is in equilibrium. At the moment of 0.4 s, the ambient temperature is unchanged and the solar radiation intensity is changed, the light intensity of unit 1 is unchanged, and the light intensity of units 2 and 3 is changed to 600 W/m², and this kind of non-uniform light condition leads to the system input power imbalance, causing the DC side voltage fluctuation, which in turn causes the modulating wave distortion. When the modulation ratio exceeds 1, the system over-modulation occurs.

Fig. 8 shows the variation curve of the DC side voltage U_{pvx} of each unit. The initial value of the open-circuit voltage is 216 V, and after MPPT control, it stabilises at the maximum power point voltage is 205 V, and the output power of the three units in the system is stabilized at 6000 W. At this stage, the system operates stably, with the peak values of the modulating waveforms of the three H-bridges maintained at 1. Additionally, the total harmonic distortion (THD) value of the system's grid-connected current is 0.83%.
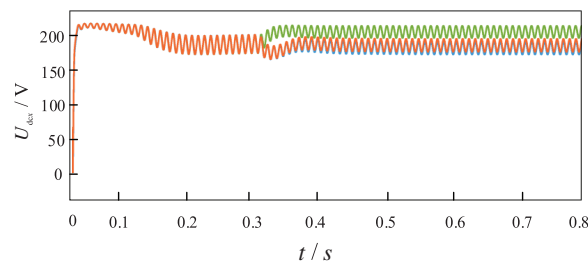
Figure 8: Schematic of injecting fundamental waves into modulated waves

At 0.4 s, the light intensity changes abruptly, causing the system entering a state of power imbalance. At this moment, the DC-side voltages of Unit 1, Unit 2, and Unit 3 stabilize at 218, 182, and 180 V, respectively. The corresponding output powers are 5070, 3175, and 3170 W, respectively, representing a significant decrease in output power compared to the normal operating state.

Fig. 9 illustrates the modulation waveform of the single-phase cascade H-bridge, using the A-phase as an example. The modulation waveform of Module 1 reaches a peak value of 1 during normal operation. However, over-modulation occurs after 0.4 s when the light intensity changes, resulting in a modulation ratio of 1.17. At this point, the system experiences over-modulation. In contrast, the modulation waveforms of Modules 2 and 3 do not exhibit over-modulation after 0.4 s, with their peak values reaching 0.89.
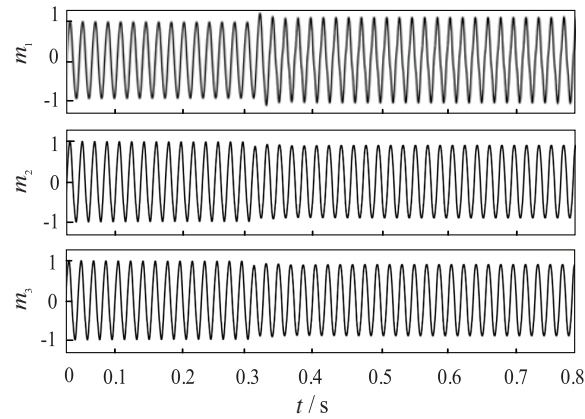
Figure 9: Modulation waveform of single-phase cascaded H-bridge

When the system does not implement any power control strategy, the grid-connected current waveform is illustrated in Fig. 10. Under constant light intensity, the Total Harmonic Distortion (THD) of the grid-connected current is 0.83%. Over-modulation occurs at 0.4, and after 0.8 s, the grid-connected current reaches 5.33%, which is abnormal and does not meet the requirements for grid connection.
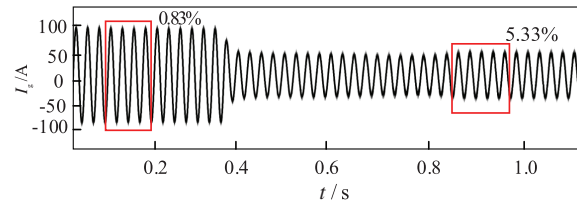

Figure 10: THD value of grid-connected current without control strategy

According to Fig. 11, it can be obtained that the sudden change in light causes the system to over-modulate after 0.4 s. The modulation ratio at this time is 1.17. The 3rd and 5th harmonic injection methods are used to reduce the modulating wave crests at 0.4 s. The modulated current THD value is reduced to 3.22% compared to that without the harmonic injection strategy. The THD value of the system's grid-connected current is reduced to 3.22% after 0.8 s compared to that without the harmonic injection strategy.
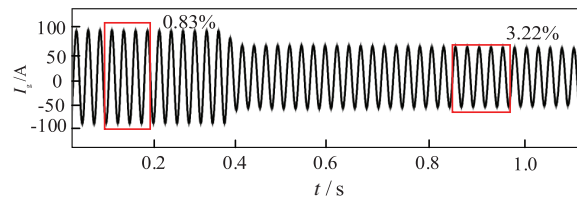

Figure 11: THD value of grid-connected current with third and fifth harmonic injection

When the improved harmonic compensation control strategy proposed in this paper is adopted, the 3rd and 5th harmonics are injected into the over-modulation module, while the inverse harmonics are injected into the unmodulated module, while so that the peak value of the modulating wave of each module is just 1, and finally the inverse triangular trapezoidal wave is injected. At this time, the grid-connected current waveform is shown in Fig. 12, from which it can be seen that the THD value of the grid-connected current

has decreased significantly compared with that of the grid-connected current that adopts the 3rd and 5th harmonic injection control strategy, and the harmonic distortion value of the current stabilises at 2.00% at around 0.8 s.
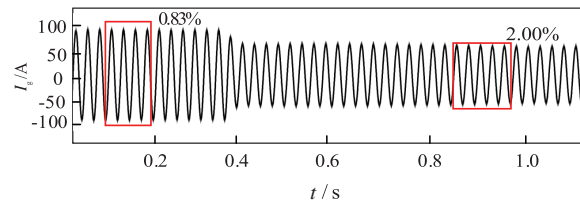

Figure 12: Current THD value using the improved power balance control strategy

Fig. 13 depicts the comparison of THD values of grid-connected currents between the existing and proposed power balancing control strategies. The comparison in the figure shows that the fusion control strategy proposed in this paper significantly optimises the harmonic performance. Compared with the system without balancing strategy, the new method thoroughly improves the waveform quality; compared with the traditional third and fifth harmonic injection schemes, the additional inclusion of inverse triangular trapezoidal wave effectively suppresses the specific subharmonic amplification problem, resulting in smaller current distortion.
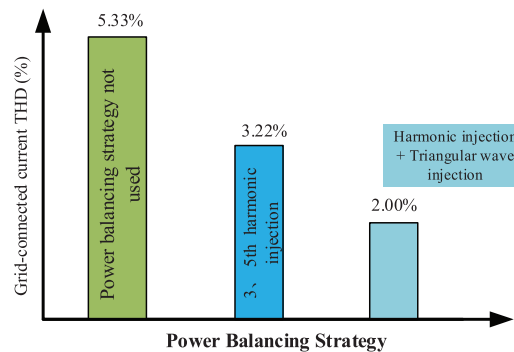

Figure 13: Comparison of THD values of grid-connected current

5 Conclusions

The improved power balance control strategy has the following advantages:

(1)   Different harmonic compensation injection strategies are used according to the range of overmodulation of the H-bridge module, which solves the overmodulation problem of the system and enables the CHB grid-connected inverter to operate stably under the input power imbalance condition.

(2)   By injecting an inverse triangular trapezoidal waveform, the waveform of the modulating waveform can be optimised to further improve the quality of the output voltage waveform, ultimately improving the quality of the grid-connected current.

The improved power balance control strategy proposed in this paper is simple, without additional hardware requirements and easy to implement.

Moreover, the proposed power balance control strategy for cascaded H-bridge inverters can be applied in many important fields:

Such as solving the power imbalance problem in photovoltaic power plants to improve the power generation efficiency; coordinating the power fluctuation of different energy sources in wind-solar-storage microgrids to enhance the stability of the system; and responding to the changes in the power grid quickly at the electric vehicle charging station to ensure the smooth charging. This strategy significantly improves the overall performance of new energy systems.

Author Contributions: The contributions to this paper are as follows: research idea and design: Feng Zhao, Haonan Xu; data collection: Haonan Xu, Xiaoqiang Chen, Ying Wang; results analysis and interpretation: Feng Zhao, Haonan Xu; first draft: Haonan Xu, Xiaoqiang Chen. All authors reviewed the results and approved the final version of the manuscript.

Availability of Data and Materials: Data is available on request from the authors. The data that support the findings of this study are available from the corresponding author, upon reasonable request.

Ethics Approval: Not applicable.

Conflicts of Interest: The authors declare no conflicts of interest to report regarding the present study.

Nomenclatures

$V_{\mathrm{PV}x}$ $I_{\mathrm{PV}x}$	Output voltage and output current of the PV module
C_x	Filter capacitor
$I_{\mathrm{H}x}$ $U_{\mathrm{dc}x}$	DC side current and voltage
$U\mathrm{H}x$	AC output voltage
Ug Ig	Grid voltage and grid current
L_{S}	Filter inductor
P_{xmax}	Maximum output power (W)
U_{oc}	Open circuit voltage (V)
U_{mpp}	Maximum power point voltage (V)
I_{mpp}	Maximum power point current (A)
I_{sc}	Short-circuit current (A)

References

1. Jia K, Gu C, Xuan Z, Li L, Lin Y. Fault characteristics of large-scale photovoltaic power plant pooling system and its line protection. J Electrotechnol. 2017;32(9):189–98. (In Chinese). doi:10.19595/j.cnki.1000-6753.tces.2017.09.022.

2. Lashab A, Sera D, Hahn F, Camurca L, Terriche Y, Liserre M, et al. Cascaded multilevel PV inverter with improved harmonic performance during power imbalance between power cells. IEEE Trans Ind Appl. 2020;56(3):2788–98. doi:10.1109/TIA.2020.2978164.

3. Aguilera RP, Acuna P, Yu Y, Konstantinou G, Townsend CD, Wu B, et al. Predictive control of cascaded H-bridge converters under unbalanced power generation. IEEE Trans Ind Electron. 2017;64(1):4–13. doi:10.1109/TIE.2016.2605618.

4. Mahfuz-Ur-Rahman AM, Islam MR, Muttaqi KM, Sutanto D. A magnetic-linked multilevel active neutral point clamped converter with an advanced switching technique for grid integration of solar photovoltaic systems. IEEE Trans Ind Appl. 2020;56(2):1990–2000. doi:10.1109/TIA.2020.2965915.

5.   Mahfuz-Ur-Rahman AM, Islam MR, Muttaqi KM, Sutanto D. An advance modulation technique for single-phase voltage source inverter to integrate SMES into low-voltage distribution. IEEE Trans Appl Supercond. 2019;29(2):1–5. doi:10.1109/TASC.2018.2882381.

6.   Wang M, Zhang X, Zhao T, Ma M, Hu Y, Wang F, et al. Harmonic compensation strategy for single-phase cascaded H-bridge PV inverter under unbalanced power conditions. IEEE Trans Ind Electron. 2020;67(12):10474–84. doi:10.1109/TIE.2019.2962461.

7.   Zhao T, Zhang X, Mao W, Wang M, Wang F, Wang X, et al. Harmonic compensation strategy for extending the operating range of cascaded H-bridge PV inverter. IEEE J Emerg Sel Top Power Electron. 2020;8(2):1341–50. doi:10.1109/JESTPE.2019.2895113.

8.   Zhao T, Chen D. A power adaptive control strategy for further extending the operation range of single-phase cascaded H-bridge multilevel PV inverter. IEEE Trans Ind Electron. 2022;69(2):1509–20. doi:10.1109/TIE.2021.3060646.

9.   Yuan Y, Zhu Q, Lu S, Liu W, Zhang Z. A cascaded H-bridge photovoltaic grid-connected inverter control strategy based on harmonic compensation. Power Autom Equip. 2022;42(12):94–100. (In Chinese). doi:10.1109/appeec.2009.4918598.

10. Wu F, Liu R, Xie Y, Lyu J. A modified power decoupling control strategy for a grid-connected inverter with a low switching frequency under unbalanced grid voltages. Energy Rep. 2022;8:757–68. doi:10.19635/j.cnki.csu-epsa.001192.

11. Chowdhury MR, Rahman MA, Islam MR, Mahfuz-Ur-Rahman AM. A new modulation technique to improve the power loss division performance of the multilevel inverters. IEEE Trans Ind Electron. 2020;68(8):6828–39. doi:10.1109/TIE.2020.3020013.

12. Sun X, Liu X, Teng J, Zhang Y, Zhao W, Li X, et al. Power balancing strategy of cascaded H-bridge photovoltaic inverter based on hybrid configuration of optical storage. Chin J Electr Eng. 2024;44(5):1948–62. (In Chinese). doi:10.13334/j.0258-8013.pcsee.223461.

13. Ye M, Cui H, Song G, Pan T, Han X. Research on power balance control strategy of three-phase CHB multilevel photovoltaic grid-connected inverter. J Power Syst Autom. 2019;31(12):49–54. (In Chinese). doi:10.19635/j.cnki.csu-epsa.000212.

14. Li J, Chen J, Gong C, He Q. A control strategy to improve the power imbalance operation capability of cascaded H-bridge inverters. J Electrotechnol. 2023;38(10):2731–43. (In Chinese). doi:10.19595/j.cnki.1000-6753.tces.220762.

15. Wang X, Li Y, Li J, Ding Y, Xue S. HCSY-MG power balance control strategy based on trapezoidal wave compensation and power adaption. Chin J Electr Eng. 2025;45(7):2645–57. (In Chinese). doi:10.13334/j.0258-8013.pcsee.232214.

16. Haq S, Biswas SP, Hosain MK, Rahman MA, Islam MR, Jahan S. A modular multilevel converter with an advanced PWM control technique for grid-tied photovoltaic system. Energies. 2021;14(2):331. doi:10.3390/en14020331.